THE JOURNAL OF BIOLOGICAL CHEMISTRY VOL. 290, NO. 26, pp. 16088–16098, June 26, 2015

Dual Effect of Phosphate Transport on Mitochondrial Ca^{2+} Dynamics*

Received for publication, November 25, 2014, and in revised form, May 6, 2015 Published, JBC Papers in Press, May 11, 2015, DOI 10.1074/jbc.M114.628446

An-Chi Wei, Ting Liu, and Brian O'Rourke[1]

From the Division of Cardiology, Department of Medicine, The Johns Hopkins University, Baltimore, Maryland 21205

Background: Inorganic phosphate (P_i) buffers matrix Ca^{2+}, but its impact on mitochondrial Ca^{2+} handling is often overlooked.
Results: Mitochondrial Ca^{2+} uptake and buffering strictly depend on anion transport rates; ATP accelerates P_i-independent Ca^{2+} uptake.
Conclusion: Maximal Ca^{2+} uniporter rate and Ca^{2+} buffering are anion transport limited; ATP alters influx without being hydrolyzed.
Significance: P_i transport is fundamentally important in controlling mitochondrial Ca^{2+} signals.

The large inner membrane electrochemical driving force and restricted volume of the matrix confer unique constraints on mitochondrial ion transport. Cation uptake along with anion and water movement induces swelling if not compensated by other processes. For mitochondrial Ca^{2+} uptake, these include activation of countertransporters (Na^+/Ca^{2+} exchanger and Na^+/H^+ exchanger) coupled to the proton gradient, ultimately maintained by the proton pumps of the respiratory chain, and Ca^{2+} binding to matrix buffers. Inorganic phosphate (P_i) is known to affect both the Ca^{2+} uptake rate and the buffering reaction, but the role of anion transport in determining mitochondrial Ca^{2+} dynamics is poorly understood. Here we simultaneously monitor extra- and intra-mitochondrial Ca^{2+} and mitochondrial membrane potential ($\Delta\Psi_m$) to examine the effects of anion transport on mitochondrial Ca^{2+} flux and buffering in P_i-depleted guinea pig cardiac mitochondria. Mitochondrial Ca^{2+} uptake proceeded slowly in the absence of P_i but matrix free Ca^{2+} ($[Ca^{2+}]_{mito}$) still rose to ~50 μM. P_i (0.001–1 mM) accelerated Ca^{2+} uptake but decreased $[Ca^{2+}]_{mito}$ by almost 50% while restoring $\Delta\Psi_m$. P_i-dependent effects on Ca^{2+} were blocked by inhibiting the phosphate carrier. Mitochondrial Ca^{2+} uptake rate was also increased by vanadate (V_i), acetate, ATP, or a non-hydrolyzable ATP analog (AMP-PNP), with differential effects on matrix Ca^{2+} buffering and $\Delta\Psi_m$ recovery. Interestingly, ATP or AMP-PNP prevented the effects of P_i on Ca^{2+} uptake. The results show that anion transport imposes an upper limit on mitochondrial Ca^{2+} uptake and modifies the $[Ca^{2+}]_{mito}$ response in a complex manner.

Mitochondrial Ca^{2+} plays a central role in regulating cellular energy supply, redox balance and cell death (1, 2) yet many questions remain about the determinants of mitochondrial Ca^{2+} flux, including the full complement of molecular components (2), signaling pathways affecting influx or efflux (2), and mitochondrial free Ca^{2+} concentrations during low and high work conditions. Accurate determination of matrix Ca^{2+} is particularly important in the heart, where workload continuously varies, accompanied by dynamic changes in ATP hydrolysis rate, Ca^{2+}, and phosphate (P_i).[2]

P_i transport through the phosphate carrier (PiC) is fundamental for oxidative phosphorylation and affects the pH gradient across the inner membrane with the effective co-transport of protons. A less appreciated function of P_i is its obligatory role in modulating mitochondrial Ca^{2+} fluxes. The earliest descriptions of mitochondrial Ca^{2+} uptake/binding (3–5) noted that ATP, P_i, and Mg^{2+} could potentiate Ca^{2+} accumulation by mitochondria, but the mechanism by which these modulators acted was unclear. P_i has been reported to affect mitochondrial Ca^{2+} in several ways, including modulation of Ca^{2+} influx, efflux, and buffering. The conventional view is that P_i transport facilitates Ca^{2+} influx by dissipating the pH gradient that builds up during Ca^{2+} entry as the protonmotive force redistributes from $\Delta\Psi_m$ to ΔpH upon stimulation of proton pumping (6). After entry, P_i then participates in dynamically buffering matrix Ca^{2+} by the formation of Ca-P_i complexes (7), to clamp mitochondrial Ca^{2+} ($[Ca^{2+}]_{mito}$) at a fixed level (8). This not only permits further Ca^{2+} uptake but also renders efflux through the mitochondrial Na^+/Ca^{2+} exchanger (mNCE) independent of total matrix Ca^{2+} load (7). The complex nature and impact of P_i, nucleotides, or other anions on mitochondrial Ca^{2+} dynamics is incompletely understood. Because of the restricted volume of the mitochondrial matrix, compensation for the electrophoretic entry of cations is a thermodynamic requirement. The PiC is regarded as an antiporter of $H_2PO_4^-/OH^-$, equivalent to a symport of $H_2PO_4^-/H^+$ (9, 10) and co-transport of protons has been noted to be an important feature of anions

* This work was supported by National Institutes of Health Grants R01HL101235 and R01HL108917. The authors declare that they have no conflicts of interest with the contents of this article.
[1] To whom correspondence should be addressed: Division of Cardiology, Dept. of Medicine, The Johns Hopkins University, 720 Rutland Ave, 1060 Ross Bldg., Baltimore, MD 21205-2195. Tel.: 410-614-0034; Fax: 410-502-5055; E-mail: bor@jhmi.edu.

[2] The abbreviations used are: P_i, inorganic phosphate; V_i, inorganic vanadate; mPTP, mitochondrial permeability transition pore; RaM, rapid uptake mode; MCU, mitochondrial Ca^{2+} uniporter; PiC, phosphate carrier; ANT, adenine nucleotide translocase; AMP-PNP, 5′-adenylyl imidodiphosphate; TMRM, tetramethylrhodamine methyl ester.

that are most effective at facilitating mitochondrial Ca^{2+} uptake (11, 12).

In a recent study in which PiC (SLC25A3) was knocked out in a cardiac-specific manner (13), mitochondrial permeability transition pore (mPTP) activation by Ca^{2+} was decreased and Ca^{2+}-induced cell death was blunted. However, in that study, some residual P_i uptake was present, and it was not determined if the maximal mitochondrial Ca^{2+} uniporter (MCU) rate in the absence of mPTP opening was altered. In contrast, another recent study showed no effect of knockdown of SLC25A3 on mitochondrial Ca^{2+} loading capacity or mPTP sensitivity but an increased cardiac hypertrophic response to pressure overload (14). Other P_i transporters also exist on the mitochondrial inner membrane. The Ca^{2+}-activated ATP-Mg/P_i carrier, SLC25A23, exchanges MgATP for P_i (15), and, in a recent study, it was proposed that SLC25A23 interacts with MCU and another accessory protein, MICU1, to regulate mitochondrial Ca^{2+} uptake, as evidenced by reduced mitochondrial Ca^{2+} uptake after knockdown of SLC25A23 (16).

Several modes of mitochondrial Ca^{2+} uptake have been reported in previous work. In addition to the main MCU-mediated uptake, a rapid uptake mode (RaM), activating and inactivating during rapid increases in Ca^{2+} near the mitochondria has been reported (17, 18). In addition, we have noted two slow MCU modes of uptake in cardiac mitochondria that displayed different Ca^{2+} affinities and Ru360 sensitivities (8), which were also modulated differentially by P_i. Mode 1 had a high Ca^{2+} affinity and low Ru360 sensitivity, while mode 2, comprising the bulk of mitochondrial Ca^{2+} uptake, was inhibited by low Ru360 concentrations (8). Extramitochondrial P_i enhanced mitochondrial Ca^{2+} accumulation through mode 1 but resulted in almost complete buffering of Ca^{2+} entry through mode 2. Interestingly, we found that mPTP opening was independent of $[Ca^{2+}]_{mito}$ but was dependent on total mitochondrial Ca^{2+} load, leading us to postulate that Ca-P_i complex accumulation was the trigger for activation of the pore.

To better understand the role of P_i in modulating mitochondrial Ca^{2+} dynamics, here we utilize P_i-depleted, isolated cardiac mitochondria to directly study the role of anions in mitochondrial Ca^{2+} uptake and buffering while monitoring changes in $\Delta\Psi_m$. We show that mitochondrial Ca^{2+} uptake occurs through both P_i-independent and P_i-dependent pathways, the latter of which could be blocked by inhibition of the PiC. Substitution of other anions led to differential effects on Ca^{2+} uptake and buffering, and revealed a novel action of adenine nucleoside trisphosphates in a non-hydrolytic role.

Experimental Procedures

Guinea pig heart mitochondria were isolated using a homogenization protocol on ice, as previously described (19). The homogenized heart suspension was centrifuged in the isolation solution (75 mM sucrose, 225 mM mannitol, 1 mM HEPES, and 1 mM EGTA, pH 7.4) at 480 g for 10 min at 4 °C, and the resulting supernatant was centrifuged at 7,700 × *g* for 10 min. The mitochondrial pellet was washed at 7,700 × *g* for 6 min and re-suspended in isolation solution at a concentration of ~20 mg/ml. The protein concentration of isolated mitochondria was determined using the BCA (bicinchoninic acid assay) method.

Endogenous phosphate in the isolated cardiac mitochondria was depleted by utilizing the hexokinase reaction with 0.75 units/ml hexokinase, 1 mM glucose, 0.5 mM ADP, 1 mM $MgCl_2$, and 5 mM glutamate/malate in 37 °C for 5 min, as previously described (20).

Mitochondria (0.5 mg) were suspended in 2 ml of a potassium-based buffer solution without phosphate (137 mM KCl, 20 μM EGTA, 20 mM HEPES, 5 mM NaCl, 1 μM CsA, and 5 mM glutamate/malate at pH 7.2). Multiple mitochondrial parameters were simultaneously monitored using a wavelength-scanning fluorometer (QuantaMaster; Photon Technology International) at room temperature. The extra-mitochondrial calcium (Ca^{2+}_{out}) was measured with 50 μM CaGreen-5N, hexapotasssium salt (505 nm ex.: 535 nm em.). Fura-FF-AM (20 μM fura-FF was incubated for 30 min at room temperature beforehand) was used to monitor intra-mitochondrial calcium (Ca^{2+}_{mito}) (340 nm/380 nm ex.: 510 nm em.). Mitochondrial membrane potential ($\Delta\Psi_m$) was monitored by the ratiometric method with 300 nM tetramethylrhodamine methyl ester (TMRM) (546 nm/573 nm ex.: 590 nm em.), and mitochondria swelling was monitored by 90 degree light scattering (540 nm ex.), as previously described (8, 21).

To measure mitochondrial pH, the succinimidyl ester form of carboxy-SNARF-1 (Life Technologies, Inc.) was loaded into Pi-depleted isolated mitochondria (incubating 30 μM for 30 min at room temperature), then washed twice and resuspended in sucrose-based isolation solution. During the measurement (520 nm ex.: 580/680 nm em.), 0.5 mg of mitochondria were suspended in 2 ml of KCl-based buffer solution without phosphate. The SNARF-1 signal was calibrated in buffer solutions with different pH values (pH 6–8) in the presence of 1 μM FCCP, 20 μg oligomycin, and 10 μM nigericin.

Results

Effects of Acute P_i Addition on Mitochondrial Ca^{2+} Dynamics—In zero P_i buffer solution, mitochondrial Ca^{2+} uptake from the cuvette upon addition of 35 μM Ca^{2+} (which increases free Ca^{2+} in the cuvette to 7 μM after binding to Ca^{2+} buffers present in the solution; Fig. 1*A*; 120–240 s) was slow and incomplete; nevertheless, $[Ca^{2+}]_{mito}$ increased monotonically to 50 μM. Acute addition of 1 mM phosphate to the buffer (at 240 s; black trace) resulted in an immediate acceleration of Ca^{2+} uptake from the cuvette, but, paradoxically, a decrease in $[Ca^{2+}]_{mito}$ to ~27 μM (Fig. 1*B*; *black trace*). The P_i effect on Ca^{2+} uptake was concentration-dependent and approached a maximum rate at 0.1 mM phosphate. The EC_{50} for the P_i effect on the initial linear Ca^{2+} uptake rate was 0.087 mM (Fig. 1*E*, *blue trace*). The P_i effect on buffering, reflected in an increase in the ratio of bound/free matrix Ca^{2+} (Fig. 1*D*), had a similar P_i dependence, as did the rate of formation of the Ca^{2+}-P_i complex (EC_{50} = 0.096 mM; Fig. 1*E*, *green trace*). Mitochondrial membrane potential ($\Delta\Psi_m$) was depolarized from ~215 mV to 170 mV in the presence of Ca^{2+} without P_i (Fig. 1*C*), but when phosphate was added, the decline in $[Ca^{2+}]_{out}$ was paralleled by restoration of $\Delta\Psi_m$ to 210mV. The rate of recovery of $\Delta\Psi_m$ was linearly related to mitochondrial Ca^{2+} uptake rate (Fig. 1*F*). Mitochondrial light scattering decreased slightly upon P_i addition, indicating low amplitude mitochondrial swelling but no

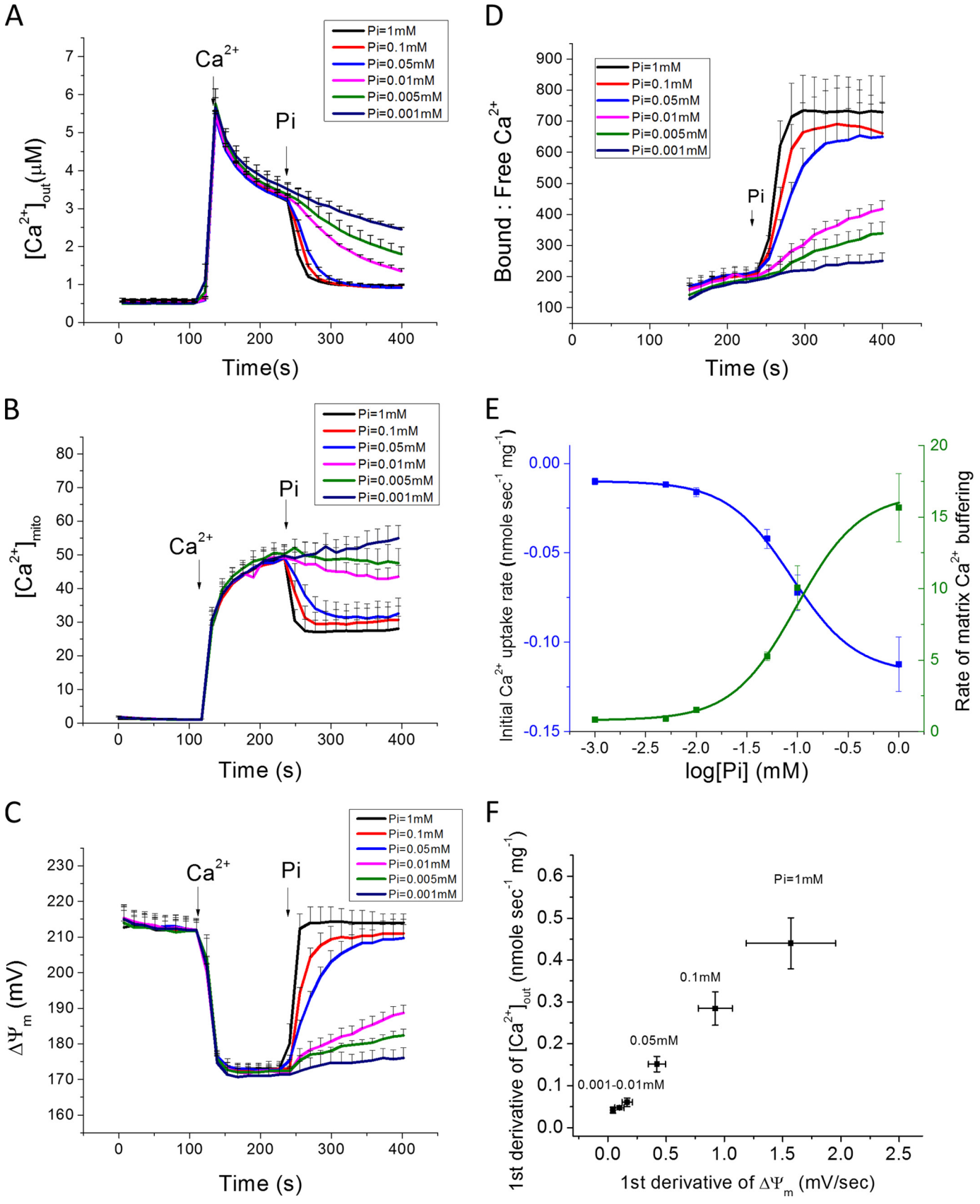
A
Pi=1mM
Pi=0.1mM
Pi=0.05mM
Pi=0.01mM
Pi=0.005mM
Pi=0.001mM
Ca2+
Pi
[Ca2+]out(μM)
Time(s)
D
Bound : Free Ca2+
Time (s)
B
[Ca2+]mito
Time (s)
E
Initial Ca2+ uptake rate (nmole sec-1 mg-1)
Rate of matrix Ca2+ buffering
log[Pi] (mM)
C
ΔΨm (mV)
Time (s)
F
1st derivative of [Ca2+]out (nmole sec-1 mg-1)
1st derivative of ΔΨm (mV/sec)
0.001-0.01mM
0.05mM
0.1mM
Pi=1mM

activation of the mitochondrial permeability transition pore (mPTP) during the experiments (data not shown).

Next, we examined the P_i effect on Ca^{2+} uptake for different Ca^{2+} additions (20–40 μM) and after adding a fixed concentration of P_i (0.1 mM; Fig. 2). Recordings of $[Ca^{2+}]_{out}$ (Fig. 2*A*), $[Ca^{2+}]_{mito}$ (Fig. 2*B*), and $\Delta\Psi_m$ (Fig. 2*C*) reveal that the P_i-dependent buffering effect takes effect above a certain threshold of matrix Ca^{2+} is reached. In the absence of P_i, $[Ca^{2+}]_{mito}$ rises to a range of 20–80 μM for total Ca^{2+} additions between 20 and 40 μM (extramitochondrial Ca^{2+} range of 1–7 μM). When phosphate is added, $[Ca^{2+}]_{mito}$ is clamped to the same steady state level (~30 μM) for any $[Ca^{2+}]_{out}$ larger than 2 μM (Fig. 2*B*). The degree of membrane potential depolarization was proportional to the amount of Ca^{2+} added to the cuvette, in accord with the size of the electrochemical gradient for Ca^{2+} across the inner membrane, the major determinant of Ca^{2+} current (Fig. 2*C*). Phase plane plots of $[Ca^{2+}]_{mito}$ *versus* $[Ca^{2+}]_{out}$ illustrates the effect of P_i to lower matrix Ca^{2+} to a similar level, despite markedly different loading histories (Fig. 2*D*, *upper panel*). In parallel, P_i transport permitted full $\Delta\Psi_m$ repolarization after various Ca^{2+} loads were accommodated (Fig. 2*D*, *lower panel*).

Mersalyl, a thiol reagent that inhibits the mitochondrial phosphate carrier (22, 23), was used to test whether phosphate regulation of mitochondrial Ca^{2+} uptake required transport through PiC (Fig. 3). Mersalyl (10 μM; blue line) partially inhibited Ca^{2+} uptake in the absence of P_i, possibly due to a partial depolarization of $\Delta\Psi_m$, yet $[Ca^{2+}]_{mito}$ still increased to the same plateau, but at a slightly slower rate. With PiC blocked, when 1 mM phosphate was added, depletion of cuvette $[Ca^{2+}]$ was not accelerated, and $[Ca^{2+}]_{mito}$ buffering did not occur, confirming that PiC-mediated P_i entry into the matrix was required for both processes.

As we previously reported (8), high capacity (mode 2) Ca^{2+} uptake is blocked by a low concentration (50 nM) of Ru360 (Fig. 4*A*), leaving only mode 1 uptake, detected by the rise in matrix Ca^{2+} (Fig. 4*B*). Inhibiting PiC with mersalyl (10 μM) had little effect on the rate of mode 1 Ca^{2+} uptake, suggesting that mode 1 uptake is P_i-independent; however, mersalyl still inhibited the effect of P_i on matrix Ca^{2+} buffering and $\Delta\Psi_m$ recovery (Fig. 4*C*).

Lehninger (11) previously reported that respiration-dependent Ca^{2+} uptake by mitochondria depends on anion transport across the inner mitochondrial membrane, supported only by permeant anions that were also capable of transporting a proton. Acetate anion is transported as the weak acid by passive diffusion with the concomitant release of a proton in the matrix. Acetate (1 mM) was capable of increasing the Ca^{2+} uptake rate in P_i-depleted mitochondria (Fig. 5, *blue traces*), albeit at a slower rate than a similar concentration of P_i, most likely due to the slow rate of acetate diffusion across the inner membrane. Increasing the acetate concentration to 30 mM accelerated the initial Ca^{2+} uptake rate to a level close to that of P_i (Fig. 5, *red traces*), with much smaller effects on matrix Ca^{2+} buffering. The acetate effect on Ca^{2+} uptake was not sustained as well as that of P_i, and was associated with slow depolarization following the initial repolarization phase. The acetate effect was not inhibited by mersalyl treatment (data not shown). Vanadate, a P_i analog, accelerated Ca^{2+} uptake in a manner similar to phosphate, and also strongly supported matrix Ca^{2+} buffering to decrease $[Ca^{2+}]_{mito}$ (Fig. 5, *green traces*). Notably, mitochondrial Ca^{2+} uptake in the presence of vanadate was not accompanied by restoration of $\Delta\Psi_m$, probably due to inhibition of OxPhos by vanadate (24). This finding argues against the idea that the anion-dependent acceleration of Ca^{2+} uptake is secondary to an increase in electrochemical driving as ΔpH is converted to $\Delta\Psi_m$ (20).

To explore this in more detail, we measured mitochondrial matrix pH ratiometrically (SNARF-1) using the same protocol of Ca^{2+} addition followed by anion addition in P_i-depleted mitochondria (Fig. 6). Prior to Ca^{2+} addition, baseline matrix pH was ~7.75 with extramitochondrial pH buffered at 7.2. Ca^{2+} addition in the absence of P_i resulted in matrix acidification to ~7.6. Therefore, ΔpH decreased, rather than increased, during P_i-independent Ca^{2+} uptake, which could have been due to displacement of protons from matrix Ca^{2+} binding sites or the coupling of Ca^{2+} entry to Na^+/Ca^{2+} and Na^+/H^+ exchange activity. The addition of P_i, V_i, or acetate led to a further decrease in pH to 7.35 during the phase of $\Delta\Psi_m$ recovery (Fig. 6). The lack of increase in ΔpH in P_i-depleted mitochondria during Ca^{2+} uptake, and the similar effects of the 3 anions on matrix pH despite differences in the extent of $\Delta\Psi_m$ recovery (Fig. 5*C*), provides further evidence against interconversion of ΔpH to $\Delta\Psi_m$ as the primary explanation for the acceleration of MCU rate. It should also be noted that there was still ample membrane potential to drive MCU current both in the absence and presence of P_i (−170 mV *versus* −190 mV). Hence, anion entry, not matrix pH change, was the primary facilitator of Ca^{2+} uptake.

Nucleotides represent another major physiological anion, hence we investigated their possible effects on mitochondrial Ca^{2+} uptake. MgATP (1 mM) accelerated mitochondrial Ca^{2+} uptake in the absence of P_i when added after (Fig. 7*A*) or prior to (Fig. 7*B*) the Ca^{2+} addition. $[Ca^{2+}]_{mito}$ level was also decreased, indicating that MgATP could also buffer matrix Ca^{2+}. Additional experiments were carried out to further investigate the mechanism of the MgATP effect on P_i-independent mitochondrial Ca^{2+} uptake. The addition of $MgCl_2$ (1 mM) alone showed only a partial inhibitory effect on mitochondrial Ca^{2+} uptake, either in the absence or presence of P_i, and no effect on matrix buffering (Fig. 7*B*). Treating the mitochondria with oligomycin (Fig. 8*A*) did not prevent the MgATP effect, ruling out the possibility that ATP hydrolysis by the F_OF_1 ATPase could be pro-

FIGURE 1. **Concentration-dependent effects of P_i on mitochondrial Ca^{2+} uptake and buffering in cardiac mitochondria.** A single Ca^{2+} addition (35 μM total $CaCl_2$ or ~7 μM free calcium) to a suspension of P_i-depleted guinea pig cardiac mitochondria results in a slow and limited uptake from the cuvette (*A*:$[Ca^{2+}]_{out}$), while matrix Ca^{2+} (*B*:$[Ca^{2+}]_{mito}$) rises with fast and slow components. Addition of various P_i concentrations (0.001–1 mM NaH_2PO_4) accelerated Ca^{2+} uptake (*A*) but decreased $[Ca^{2+}]_{mito}$ (*B*), reflecting an increase in matrix bound:free Ca^{2+} (*D*). Mitochondrial inner membrane potential ($\Delta\Psi_m$) depolarizes and recovers in parallel with the Ca^{2+} and P_i additions, respectively (*C*). *E*, concentration dependence of the P_i effect on Ca^{2+} uptake (*blue*) and buffering (*green*) rates, with saturation at ~0.1 mM P_i. *F*, linear relationship between the rate of change of $[Ca^{2+}]_{out}$ and $\Delta\Psi_m$ measured as the first derivative of the signals for first 15 s after the P_i addition. (Data in *panels A-E* represent mean ± S.E. for $n = 3$ experiments; *panel F*, $n = 5$).

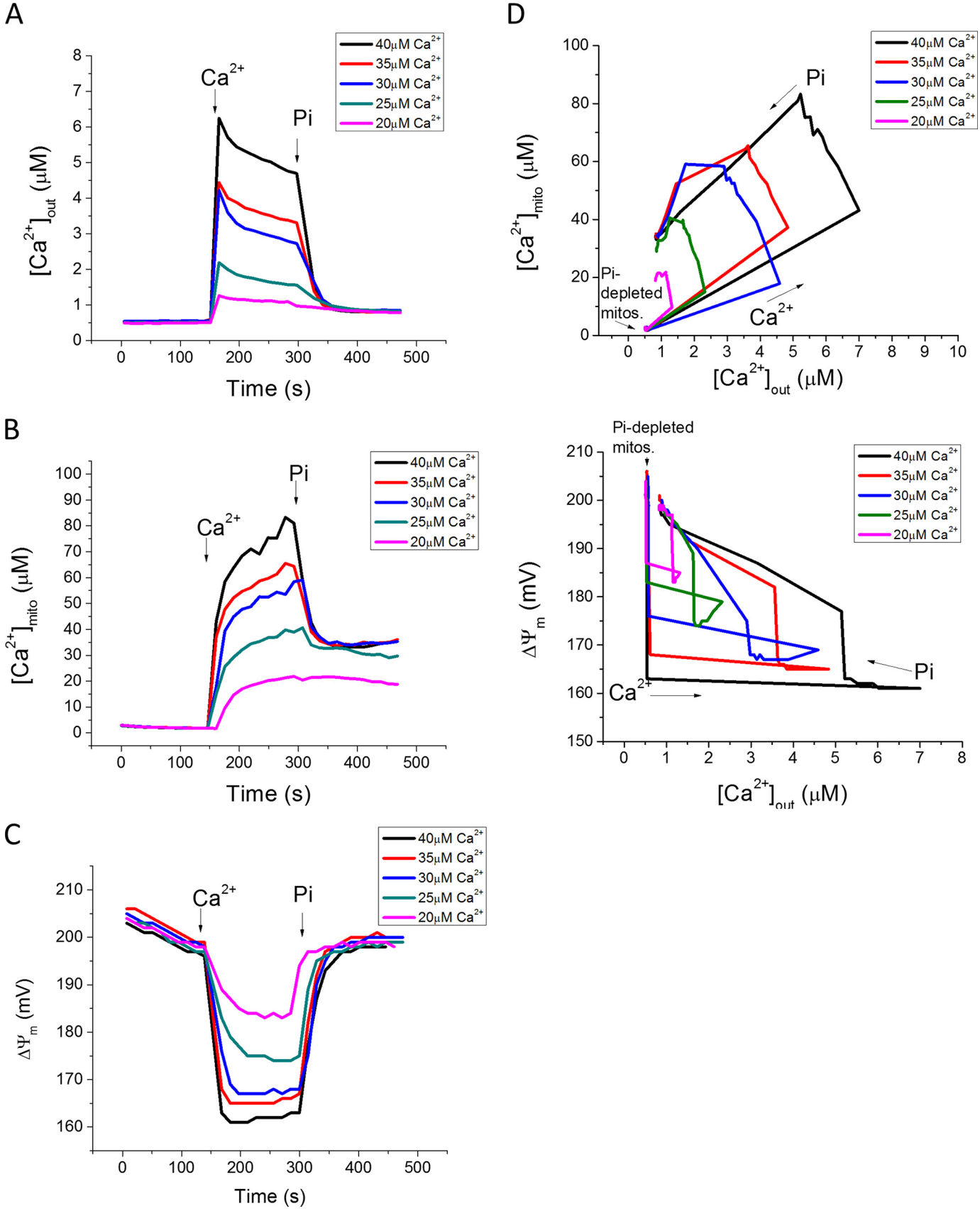

FIGURE 2. **P_i uptake is required to clamp $[Ca^{2+}]_{mito}$ to a setpoint.** *A*, Ca^{2+} additions to P_i-depleted mitochondria in the range of 20–40 μM (at 150 s) were followed by 0.1 mM P_i (at 300 s) to initiate Ca^{2+} uptake and buffering. *B*, increases in $[Ca^{2+}]_{mito}$ exceeding 30 μM in the absence of P_i were quickly clamped back to 30 μM upon P_i addition, regardless of total mitochondrial Ca^{2+} load. *C*, $\Delta\Psi_m$ changes during the protocol. *D*, phase-plane analysis of $[Ca^{2+}]_{out}$ *versus* $[Ca^{2+}]_{mito}$ (*upper*) and $[Ca^{2+}]_{out}$ *versus* $\Delta\Psi_m$ (*lower*) before and after P_i addition.

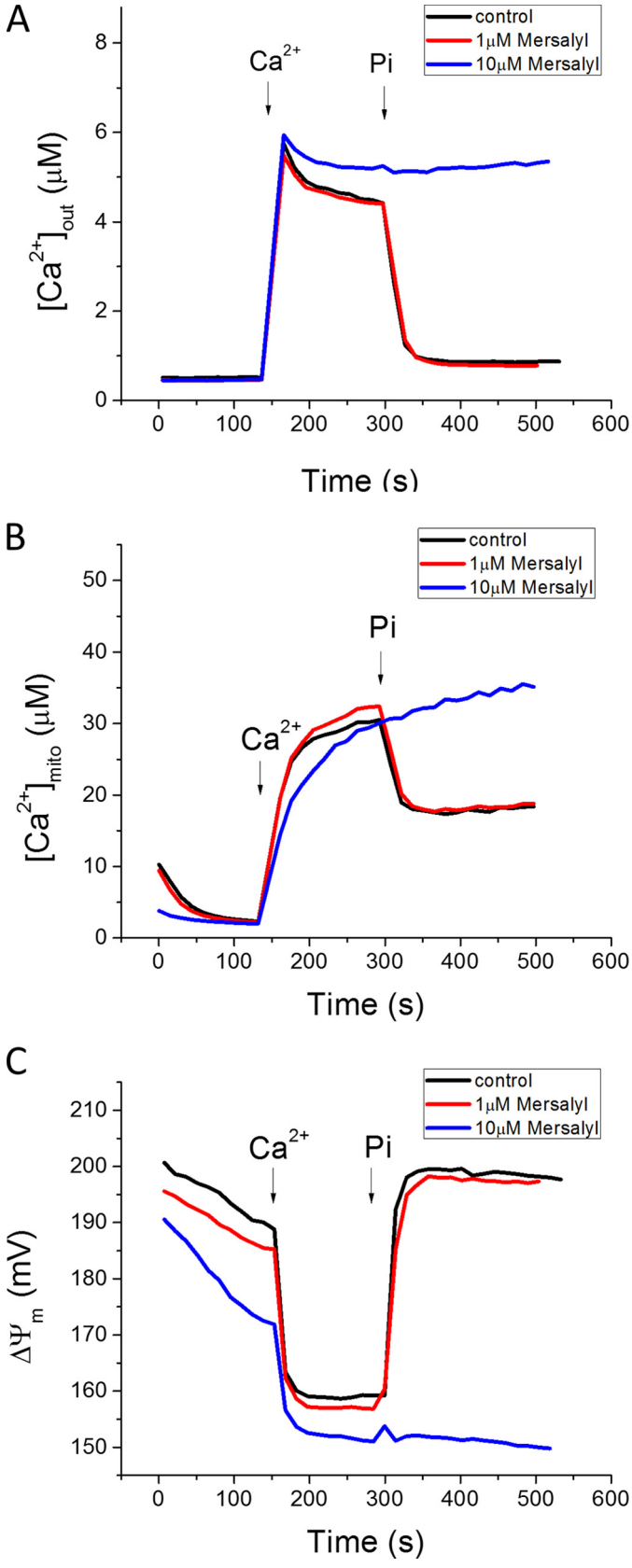

FIGURE 3. **PiC inhibition blocks acceleration of Ca^{2+} uptake and matrix Ca^{2+} buffering.** 10 μM (*blue*), but not 1 μM (*red*), mersalyl inhibited the P_i effect on mitochondrial Ca^{2+} uptake (*A*) and buffering (*B*). *C*, $\Delta\Psi_m$ was partially depolarized in the presence of 10 μM mersalyl, which may account for the somewhat slower initial P_i-independent Ca^{2+} uptake kinetics.

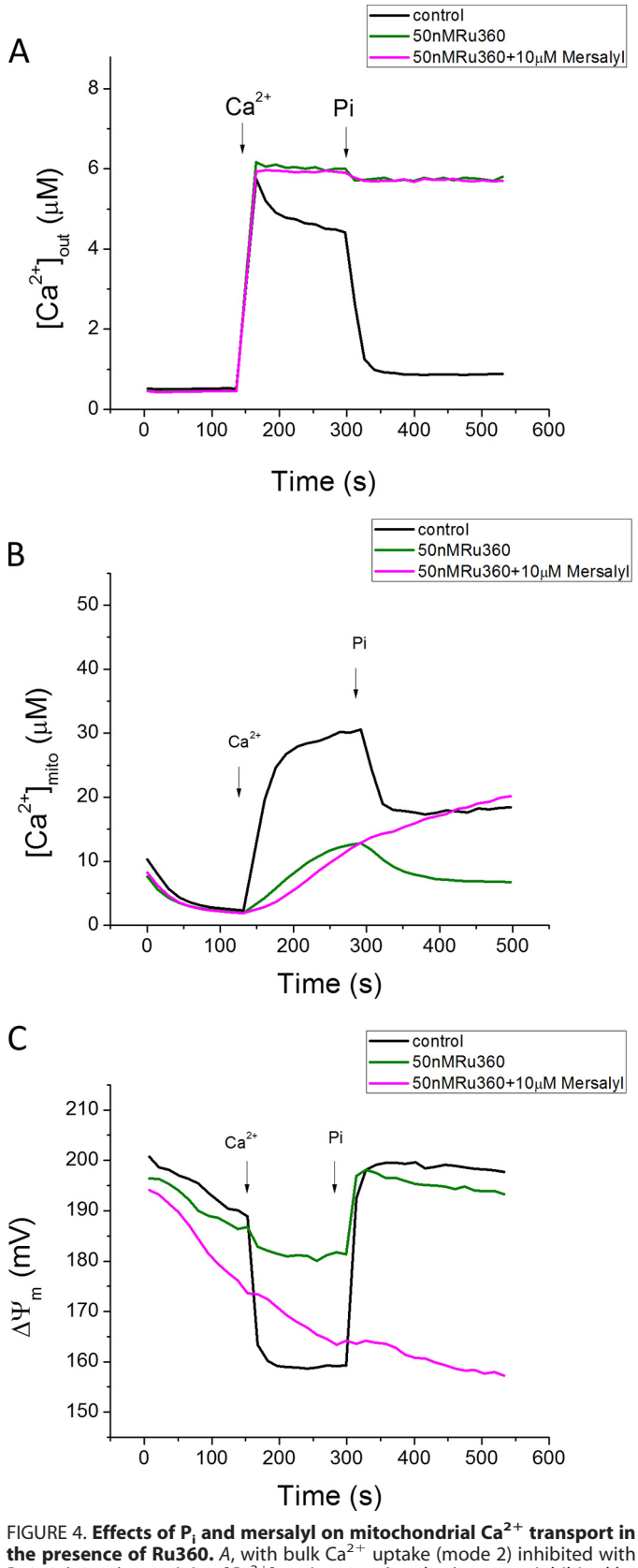

FIGURE 4. **Effects of P_i and mersalyl on mitochondrial Ca^{2+} transport in the presence of Ru360.** *A*, with bulk Ca^{2+} uptake (mode 2) inhibited with Ru360 (50 nM), remaining $[Ca^{2+}]_{mito}$ increase (mode 1) was not inhibited by mersalyl, although the P_i effect on buffering was still blocked (*B*). *C*, $\Delta\Psi_m$ responses.

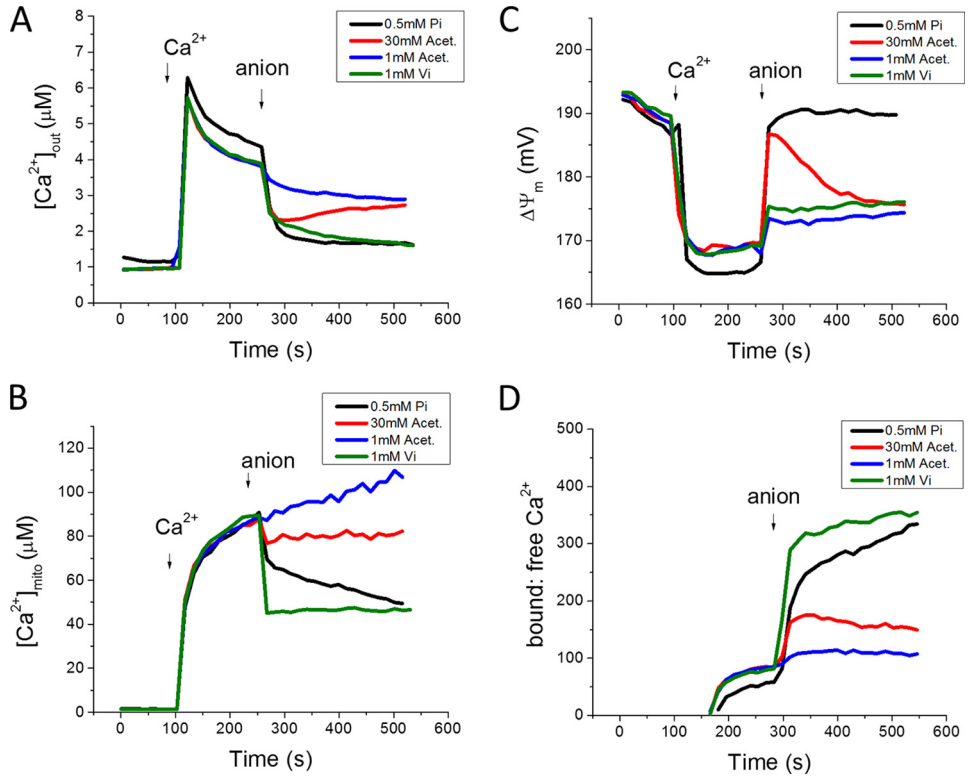

FIGURE 5. **Anions acetate, vanadate, and phosphate show different effects on mitochondrial Ca^{2+} dynamics.** Phosphate (0.5 mM Pi, *black*), acetate (1, *blue* or 30 mM Acet., *red*), or vanadate (1 mM V_i, *green*) were added at 240 s to phosphate-depleted mitochondria after a 35 μM Ca^{2+} addition. $[Ca^{2+}]_{out}$ (*A*), $[Ca^{2+}]_{mito}$ (*B*), $\Delta\Psi_m$ (*C*), Ca^{2+} bound-to-free ratio (*D*).

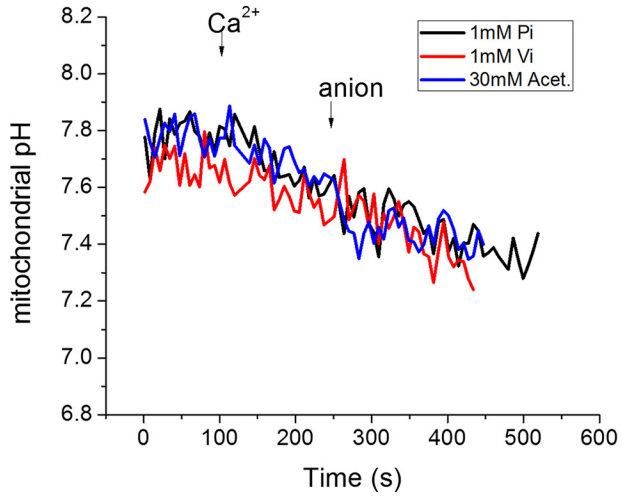

FIGURE 6. **Mitochondrial pH measurement in P_i-depleted mitochondria.** Mitochondrial pH was measured using the ratiometric pH indicator carboxy-SNARF-1. Mitochondrial pH decreased to a similar extent after the Ca^{2+} addition and after anion addition regardless which anion was used. 40 μM Ca^{2+} was first added, followed by 1 mM P_i (or 1 mM V_i or 30 mM acetate), as indicated.

viding matrix P_i. The ATP effect was also not impacted by blocking the adenine nucleotide translocase with bongkrekic acid (Fig. 8*B*) or carboxyatractyloside (data not shown), and ADP was incapable of accelerating the Ca^{2+} uptake rate (Fig. 8*B*). PiC inhibition also had no effect on the MgATP facilitation of Ca^{2+} uptake (Fig. 8*C*).

Finally, the non-hydrolyzable ATP analog, AMP-PNP, was shown to have a similar effect on mitochondrial Ca^{2+} dynamics as MgATP (Fig. 7), *i.e.* increased Ca^{2+} uptake rate and decreased $[Ca^{2+}]_{mito}$. These data indicate that ATP facilitates mitochondrial Ca^{2+} uptake through a novel direct effect of the molecule itself, presumably requiring nucleoside triphosphate uptake by a non-canonical transporter, since matrix Ca^{2+} buffering was also increased by ATP.

Discussion

The present study quantitatively investigated the fundamental role of P_i transport on mitochondrial Ca^{2+} uptake and buffering by monitoring extra- and intra-mitochondrial Ca^{2+} and $\Delta\Psi_m$. The major findings were that P_i directly facilitates mitochondrial Ca^{2+} uptake in a concentration-dependent manner while simultaneously buffering $[Ca^{2+}]_{mito}$ to a fixed setpoint. Using P_i-depleted mitochondria, a novel regulatory mechanism involving MgATP was also revealed, whereby it increased mitochondrial Ca^{2+} uptake. The MgATP effect did not require ATP hydrolysis. The results demonstrate that there is a strict dependence of maximal MCU, as well as $[Ca^{2+}]_{mito}$, on anion flux rate, highlighting the regulatory complexity of cardiac mitochondrial Ca^{2+} dynamics.

The ability of mitochondria to accumulate massive amount of Ca^{2+} has been known for more than fifty years (3, 14, 25). While previous work established that P_i increases mitochondrial Ca^{2+} loading (11, 26) and participates in mitochondrial Ca^{2+} buffering to clamp matrix Ca^{2+} at a limiting setpoint (21, 27), the dual role of P_i has not been studied quantitatively in energized cardiac mitochondria while measuring changes in total Ca^{2+} uptake, matrix Ca^{2+}, and $\Delta\Psi_m$ in parallel. The protocol used here uniquely permitted the study of both the P_i-de-

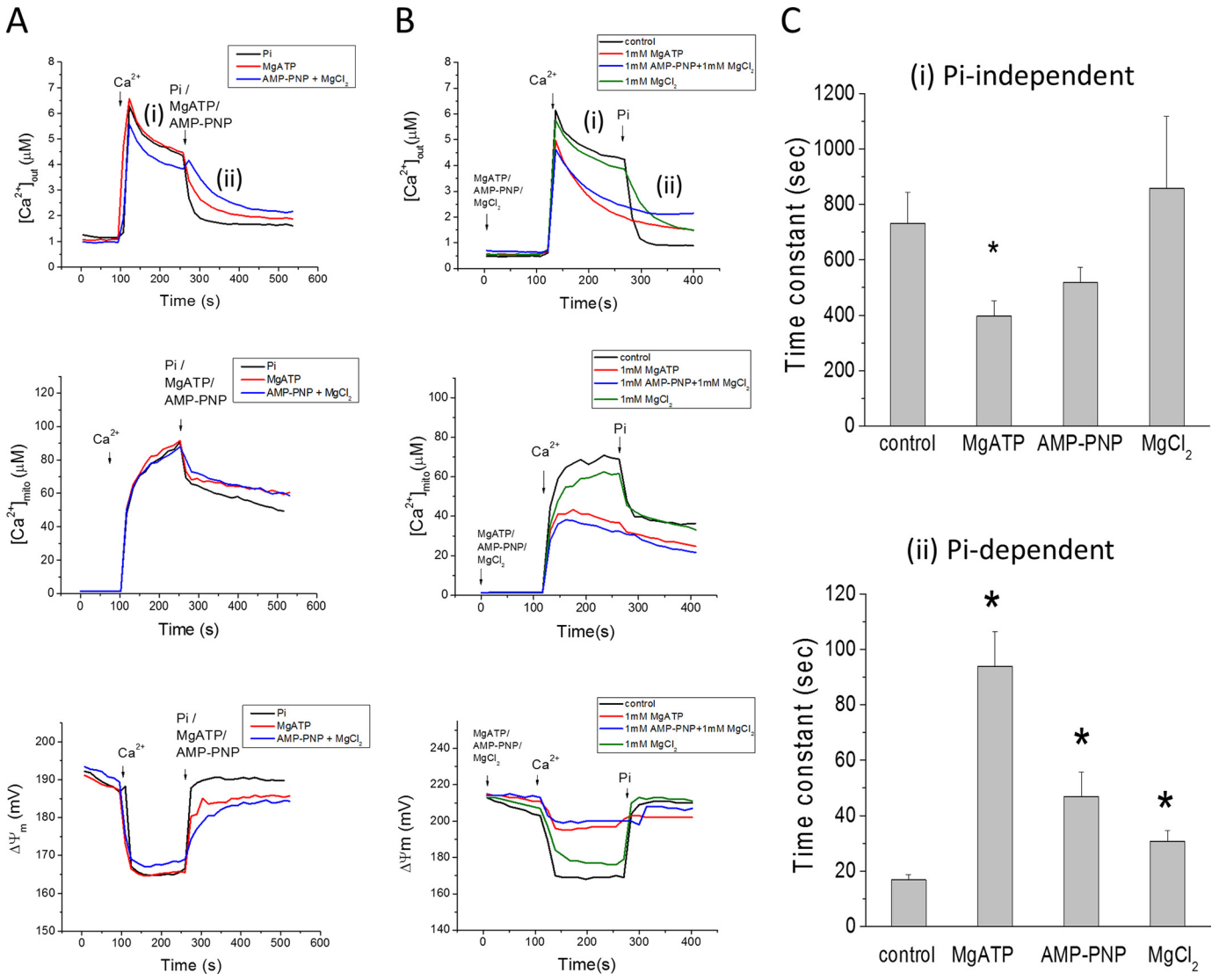

FIGURE 7. **MgATP accelerates mitochondrial Ca^{2+} uptake in P_i-depleted mitochondria.** *A*, acute addition of either 0.5 mM P_i (*black*), 1 mM MgATP(*red*), or 1 mM Li^+-AMP-PNP/$MgCl_2$ (*blue*), added after Ca^{2+}, accelerates mitochondrial Ca^{2+} uptake. Ca^{2+} (35 μM) was added at 100 s to initiate P_i-independent Ca^{2+} uptake (i); 1 mM P_i was added at 270 s to initiate the P_i-dependent phase (ii). *B*, Ca^{2+} uptake rate after pre-incubation with MgATP, AMP-PNP or $MgCl_2$, added 120 s before Ca^{2+}. Notably, P_i (1 μM) did not accelerate Ca^{2+} uptake when mitochondria were preincubated with MgATP or MgAMP-PNP. *C*, summary of the effects of MgATP, AMP-PNP or $MgCl_2$ on Ca^{2+} uptake. Data in *C* are presented as mean ± S.E. $n = 10, 8, 4$, and 4 for the 4 groups shown. *: $p < 0.05$. The kinetics of extra-mitochondrial Ca^{2+} ($[Ca^{2+}]_{out}$) from *panel B* were fitted using exponential functions to obtain time constants during the P_i-independent and P_i-dependent Ca^{2+} uptake phases. MgATP and AMP-PNP accelerated P_i-independent Ca^{2+} uptake rates, while $MgCl_2$ slightly prolonged Ca^{2+} uptake only in the presence of P_i. For phase (i), P_i-independent uptake, a double exponential was employed: $[Ca^{2+}]_{out}(t) = A_{fast}[\exp(-t/\tau_{fast}] + A_{slow}[\exp(-t/\tau_{slow})]$. A_{fast} and A_{slow} are the maximum amplitude; τ_{fast} and τ_{slow} are the time constants of the fast and slow components of exponential decay, respectively. Only the slow decay time constants are plotted for different treatments. In phase (ii), the $[Ca^{2+}]_{out}$ was fitted by a single exponential function $[Ca^{2+}]_{out}(t) = A[\exp(-t/\tau] + C$.

pendent and P_i-independent components of mitochondrial Ca^{2+}uptake and defined the efficacy of the anion for activation of uptake *versus* buffering. P_i and V_i were approximately equally effective in supporting both functions, while acetate facilitated uptake but had little effect on matrix buffering.

ATP has been shown to participate in regulating mitochondrial Ca^{2+} accumulation. It was first reported by Vasington and Murphy (3), and DeLuca and Engstrom (25) that ATP was necessary for the uptake of Ca^{2+}. In the former study, P_i or ATP enhanced, and respiratory inhibitors or uncouplers inhibited, "active" Ca^{2+} uptake, while in the latter study, it was concluded that neither P_i nor coupled respiration was required for Ca^{2+} uptake/binding (25). However, these studies did not take into account possible effects of Mg^{2+}, ATP, P_i, or even substrate availability on the electrochemical driving force for Ca^{2+} uptake (indeed, this work took place prior to wide acceptance of the chemiosmotic hypothesis). Later, Carafoli and Lehninger showed that ATP (or ADP) is taken up along with Ca^{2+} and P_i to form hydroxyapatite-like precipitates in the mitochondrial matrix. Without the uptake of ATP (or ADP), no granules were formed (5). Weinbach and Von Brandt then found that the granules contained adenine nucleotides (28). The possible co-precipitation of Ca-P_i and nucleotide was, therefore, a potential explanation of why ATP accelerated mitochondrial Ca^{2+} uptake. Our findings show that, independent of P_i, ATP, but not ADP, can regulate mitochondrial Ca^{2+} uptake and buffering, and that hydrolysis is not required. The transporter mediating this effect, and whether ATP buffers by

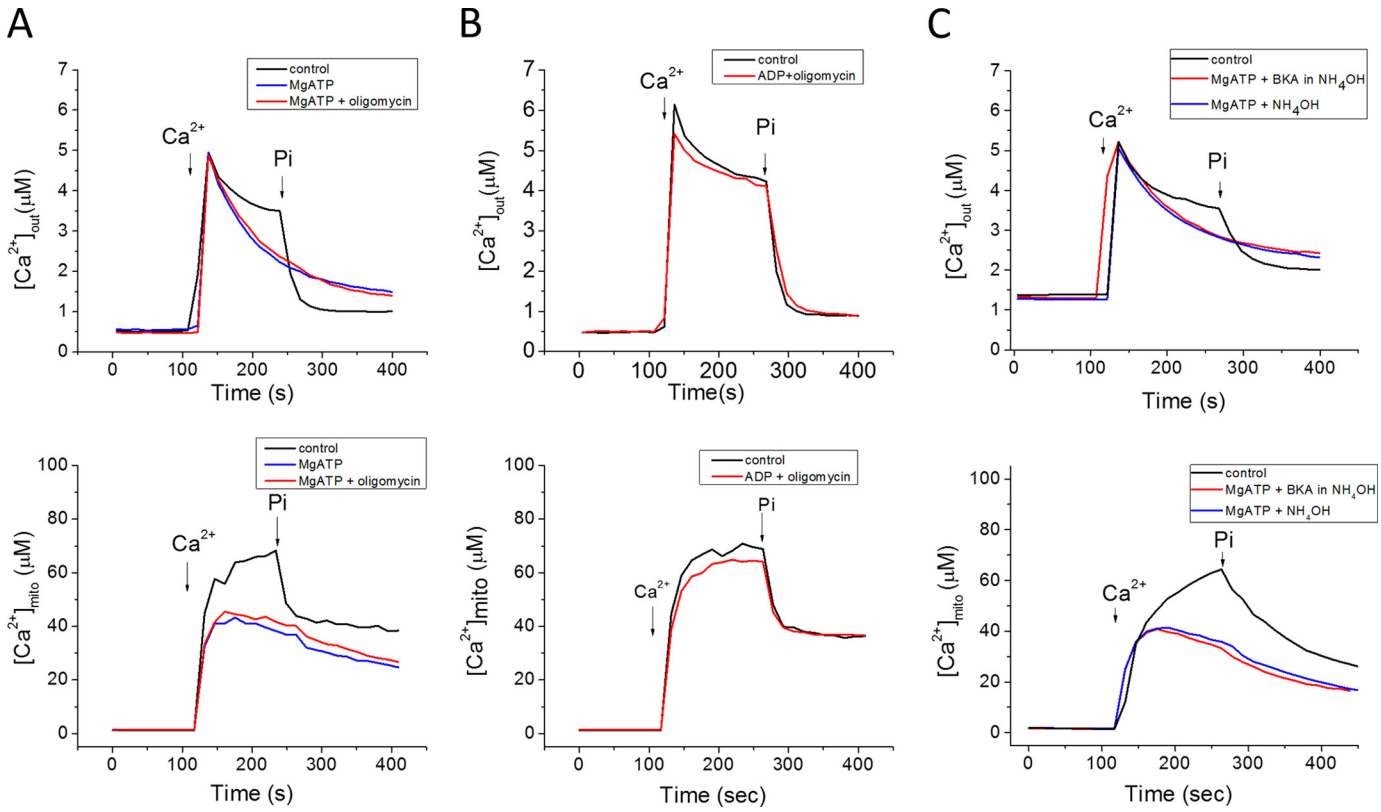

FIGURE 8. **ATP effects were not altered by inhibition of ANT or the mitochondrial ATP synthase.** *A*, oligomycin (ATP synthase inhibitor) pretreatment did not alter MgATP facilitation of P_i-independent Ca^{2+} uptake. *B*, ADP did not accelerate P_i-independent Ca^{2+} uptake. *C*, bongkrekic acid (*BKA*; ANT inhibitor) did not alter the ATP response.

forming a high affinity complex with Ca^{2+}, remains to be determined.

Recent studies have confirmed that MCU is a selective Ca^{2+} channel (29) comprised of a defined pore subunit (MCUa) (30, 31). In most studies, it is assumed that maximal MCU rates are a function of the pore's properties, regulated by accessory proteins in the Ca^{2+} uptake complex (*e.g.* MCUb (32), MICU1 and MICU2 (33–36), MCUR (37), EMRE (38)). However, our findings in intact mitochondria demonstrate that the maximal Ca^{2+} uptake rate is limited by the anion transport rate. This effect is masked under physiological conditions because P_i is usually at saturating concentrations with respect to effect on Ca^{2+} uptake (EC_{50} of P_i = 87.5 μM). Interestingly, the $[Ca^{2+}]_{mito}$ level was buffered and reached a steady state near 20–30 μM when the phosphate concentration was > 0.01 mM (Fig. 1 B) or when $[Ca^{2+}]_{out}$ level was > 2 μM (Fig. 2). This calcium-phosphate buffering effect allows estimation of the buffering threshold; however, even though the extramitochondrial phosphate concentration required for calcium buffering was ~0.01 mM, $[P_i]_{mito}$ may not necessarily be equal to $[P_i]_{out}$. In this regard, employing phosphorous NMR spectroscopy, Garlick *et al.* (39, 40) reported that mitochondrial P_i concentration was 2.5× the cytoplasmic level in intact hearts (~6 mM). In contrast, in solution, the calcium-phosphate complex only forms when calcium is in the millimolar range ($Ksp = 3 \times 10^{-30}$ for $Ca_3(PO_4)_2$) (20), a Ca^{2+} concentration at least an order of magnitude higher than we measured either outside or inside the mitochondria.

The method described here also provides an indirect way of measuring phosphate influx since the mitochondrial Ca^{2+} uptake rate is proportional to the phosphate concentration and sensitive to the phosphate carrier inhibitor. By assuming 1:1 or 1:1.5 P_i:Ca transport stoichiometry (27), we could approximate the phosphate flux to be around 0.5–1 nmol/mg/sec at 1 mM $[P_i]$, and this rate is close to the range of the reported phosphate transport rate in the rat liver mitochondria at 2 mM, which was determined by the inhibitor stop method with ^{32}P at 0 °C (41). In keeping with the overall hypothesis that anion flux limits Ca^{2+} uptake, this maximum P_i transport rate corresponded to the maximum MCU rates previously reported for guinea pig cardiac mitochondria (21).

Phosphate is known to play a role in regulating mitochondrial Ca^{2+} and function. It has previously been reported that P_i is required for bulk mitochondrial Ca^{2+} uptake (42). Possible mechanisms of phosphate facilitation of Ca^{2+} uptake could be explained by (i) precipitation of mitochondrial Ca^{2+} by forming a Ca-P_i complex to maintain the electrochemical driving force for Ca^{2+}, (ii) the requirement for co-transport of an anion via PiC with Ca^{2+} to maintain charge balance (supported by the acetate result), or (iii) direct interaction with Ca^{2+} transporters. In the current study, we confirmed that phosphate participates in clamping mitochondrial $[Ca^{2+}]_{mito}$ level to maintain a Ca^{2+} gradient for Ca^{2+} uptake. Dissipation of the proton gradient by phosphate influx was unlikely to be the main reason for enhancing Ca^{2+} uptake, since V_i could equally increase uptake without restoring $\Delta\Psi_m$ (Fig. 5*C*).

Mitochondrial matrix or extramitochondrial P_i, by themselves, were probably not direct allosteric regulators of the mitochondrial calcium uniporter because concomitant P_i influx was absolutely required to maintain fast Ca^{2+} uptake. The PiC has also been implicated in the regulation of mPTP opening to modulate cell death (13, 43); however, whether the mechanism is through a direct PiC-mPTP interaction or merely the result of a loss of P_i influx to regulate matrix Ca^{2+}, or the P_i-Ca^{2+} complex, is unclear. To verify the importance of P_i in regulating mitochondrial Ca^{2+} dynamics, further testing on PiC knockdown cells or animals (13, 16) would be helpful to understand the molecular basis of the P_i-dependent process described herein.

Nucleotide effects on mitochondrial Ca^{2+} uptake have been reported previously (44); however, ATP or AMP-PNP were shown to inhibit the uniporter from a site on the outside of the inner membrane. Thus, the effect of ATP to increase P_i-independent Ca^{2+} uptake shown here has not been observed before. The nature of the ATP transporter involved remains to be determined, as we ruled out adenine nucleotide translocase or the ATP synthase as contributors to the mechanism. An ATP-Mg/P_i carrier (SLC25A23) has also been described in cardiac mitochondria, representing another possible anion influx pathway. Knockdown of this exchanger was recently shown to impact mitochondrial Ca^{2+} dynamics (16), but it is unclear how this ATP/P_i antiporter would be able to function in the P_i-depleted mitochondria used in the present study.

In conclusion, these findings support a major role for anion influx in determining the maximal Ca^{2+} influx rate and matrix Ca^{2+} concentration in cardiac mitochondria. P_i uptake is required for maximal enhancement of MCU rate, as well as maximal buffering capacity. ATP is not strictly required for Ca^{2+} uptake, but facilitates P_i-independent uptake (ADP does not substitute). The Ca-P_i buffer system clamps the free Ca^{2+} at an upper limit, allowing massive accumulation of Ca^{2+} without increasing the efflux rate or diminishing the electrochemical driving force for entry. The mitochondria are therefore able to regulate metabolism via Ca^{2+} sensing and also can act as a cellular Ca^{2+} sink when there is a chronic, potentially pathological, increase in extramitochondrial Ca^{2+}. Notably, we show that the first role is modulated by the P_i effect on Ca^{2+} uptake, effectively incorporating P_i, which also rises with energy demand, into the sensing process. Considering that P_i, ATP, and Ca^{2+} dynamics are altered under metabolic stress, it will be important to define how the two effects of P_i contribute to the pathophysiology of cardiac disease.

References

1. Rizzuto, R., De Stefani, D., Raffaello, A., and Mammucari, C. (2012) Mitochondria as sensors and regulators of calcium signalling. *Nat. Rev. Mol. Cell Biol.* **13,** 566–578
2. Liu, T., and O'Rourke, B. (2009) Regulation of mitochondrial Ca^{2+} and its effects on energetics and redox balance in normal and failing heart. *J. Bioenerg. Biomembr.* **41,** 127–132
3. Vasington, F. D., and Murphy, J. V. (1962) Ca ion uptake by rat kidney mitochondria and its dependence on respiration and phosphorylation. *J. Biol. Chem.* **237,** 2670–2677
4. Chance, B. (1965) The Energy-Linked Reaction of Calcium with Mitochondria. *J. Biol. Chem.* **240,** 2729–2748
5. Carafoli, E., Rossi, C. S., and Lehninger, A. L. (1965) Uptake of Adenine Nucleotides by Respiring Mitochondria during Active Accumulation of Ca++ and Phosphate. *J. Biol. Chem.* **240,** 2254–2261
6. Nicholls, D. G., and Ferguson, S. (2013) *Bioenergetics* 4th Ed., Academic Press
7. Balaban, R. S., Bose, S., French, S. A., and Territo, P. R. (2003) Role of calcium in metabolic signaling between cardiac sarcoplasmic reticulum and mitochondria *in vitro*. *Am. J. Physiol. Cell Physiol.* **284,** C285–C293
8. Wei, A. C., Liu, T., Winslow, R. L., and O'Rourke, B. (2012) Dynamics of matrix-free Ca^{2+} in cardiac mitochondria: two components of Ca^{2+} uptake and role of phosphate buffering. *J. Gen. Physiol.* **139,** 465–478
9. Wohlrab, H. (1986) Molecular aspects of inorganic phosphate transport in mitochondria. *Biochim. Biophys. Acta* **853,** 115–134
10. Krämer, R. (1996) Structural and functional aspects of the phosphate carrier from mitochondria. *Kidney Int.* **49,** 947–952
11. Lehninger, A. L. (1974) Role of phosphate and other proton-donating anions in respiration-coupled transport of Ca^{2+} by mitochondria. *Proc. Natl. Acad. Sci. U.S.A.* **71,** 1520–1524
12. Zoccarato, F., and Nicholls, D. (1982) The role of phosphate in the regulation of the independent calcium-efflux pathway of liver mitochondria. *Eur. J. Biochem.* **127,** 333–338
13. Kwong, J. Q., Davis, J., Baines, C. P., Sargent, M. A., Karch, J., Wang, X., Huang, T., and Molkentin, J. D. (2014) Genetic deletion of the mitochondrial phosphate carrier desensitizes the mitochondrial permeability transition pore and causes cardiomyopathy. *Cell Death Differ.* **21,** 1209–1217
14. Carafoli, E. (2010) The fateful encounter of mitochondria with calcium: How did it happen? *Biochim. Biophys. Acta* **1797,** 595–606
15. Fiermonte, G., De Leonardis, F., Todisco, S., Palmieri, L., Lasorsa, F. M., and Palmieri, F. (2004) Identification of the mitochondrial ATP-Mg/Pi transporter. Bacterial expression, reconstitution, functional characterization, and tissue distribution. *J. Biol. Chem.* **279,** 30722–30730
16. Hoffman, N. E., Chandramoorthy, H. C., Shanmughapriya, S., Zhang, X. Q., Vallem, S., Doonan, P. J., Malliankaraman, K., Guo, S., Rajan, S., Elrod, J. W., Koch, W. J., Cheung, J. Y., and Madesh, M. (2014) SLC25A23 augments mitochondrial Ca(2)(+) uptake, interacts with MCU, and induces oxidative stress-mediated cell death. *Mol. Biol. Cell* **25,** 936–947
17. Sparagna, G. C., Gunter, K. K., Sheu, S. S., and Gunter, T. E. (1995) Mitochondrial calcium uptake from physiological-type pulses of calcium. A description of the rapid uptake mode. *J. Biol. Chem.* **270,** 27510–27515
18. Buntinas, L., Gunter, K. K., Sparagna, G. C., and Gunter, T. E. (2001) The rapid mode of calcium uptake into heart mitochondria (RaM): comparison to RaM in liver mitochondria. *Biochim. Biophys. Acta* **1504,** 248–261
19. Wei, A. C., Aon, M. A., O'Rourke, B., Winslow, R. L., and Cortassa, S. (2011) Mitochondrial energetics, pH regulation, and ion dynamics: a computational-experimental approach. *Biophys. J.* **100,** 2894–2903
20. Chalmers, S., and Nicholls, D. G. (2003) The relationship between free and total calcium concentrations in the matrix of liver and brain mitochondria. *J. Biol. Chem.* **278,** 19062–19070
21. Wei, A. C., Liu, T., Cortassa, S., Winslow, R. L., and O'Rourke, B. (2011) Mitochondrial Ca^{2+} influx and efflux rates in guinea pig cardiac mitochondria: low and high affinity effects of cyclosporine A. *Biochim. Biophys. Acta* **1813,** 1373–1381
22. Tyler, D. D. (1969) Evidence of a phosphate-transporter system in the inner membrane of isolated mitochondria. *Biochem. J.* **111,** 665–678
23. Papa, S., Kanduc, D., and Lofrumento, N. E. (1973) Phosphate transport in mitochondria action of mersalyl on the binding and transport of inorganic phosphate. *FEBS Lett.* **36,** 9–11
24. DeMaster, E. G., and Mitchell, A. (1973) A comparison of arsenate and vanadate as inhibitors or uncouplers of mitochondrial and glycolytic energy metabolism. *Biochemistry* **12,** 3616–3621
25. Deluca, H. F., and Engstrom, G. W. (1961) Calcium uptake by rat kidney mitochondria. *Proc. Natl. Acad. Sci. U.S.A.* **47,** 1744–1750
26. Langer, G. A., and Nudd, L. M. (1980) Addition and kinetic characterization of mitochondrial calcium in myocardial tissue culture. *Am. J. Physiol.* **239,** H769–H774
27. Nicholls, D. G., and Chalmers, S. (2004) The integration of mitochondrial calcium transport and storage. *J. Bioenerg. Biomembr.* **36,** 277–281
28. Weinbach, E. C., and Von Brand, T. (1967) Formation, isolation and composition of dense granules from mitochondria. *Biochim. Biophys.*

Acta **148,** 256–266
29. Kirichok, Y., Krapivinsky, G., and Clapham, D. E. (2004) The mitochondrial calcium uniporter is a highly selective ion channel. *Nature* **427,** 360–364
30. Chaudhuri, D., Sancak, Y., Mootha, V. K., and Clapham, D. E. (2013) MCU encodes the pore conducting mitochondrial calcium currents. *Elife* **2,** e00704
31. De Stefani, D., Raffaello, A., Teardo, E., Szabò, I., and Rizzuto, R. (2011) A forty-kilodalton protein of the inner membrane is the mitochondrial calcium uniporter. *Nature* **476,** 336–340
32. Raffaello, A., De Stefani, D., Sabbadin, D., Teardo, E., Merli, G., Picard, A., Checchetto, V., Moro, S., Szabò, I., and Rizzuto, R. (2013) The mitochondrial calcium uniporter is a multimer that can include a dominant-negative pore-forming subunit. *EMBO J.* **32,** 2362–2376
33. Patron, M., Checchetto, V., Raffaello, A., Teardo, E., Vecellio Reane, D., Mantoan, M., Granatiero, V., Szabò, I., De Stefani, D., and Rizzuto, R. (2014) MICU1 and MICU2 finely tune the mitochondrial Ca^{2+} uniporter by exerting opposite effects on MCU activity. *Mol. Cell* **53,** 726–737
34. Plovanich, M., Bogorad, R. L., Sancak, Y., Kamer, K. J., Strittmatter, L., Li, A. A., Girgis, H. S., Kuchimanchi, S., De Groot, J., Speciner, L., Taneja, N., Oshea, J., Koteliansky, V., and Mootha, V. K. (2013) MICU2, a paralog of MICU1, resides within the mitochondrial uniporter complex to regulate calcium handling. *PLoS One* **8,** e55785
35. Csordás, G., Golenár, T., Seifert, E. L., Kamer, K. J., Sancak, Y., Perocchi, F., Moffat, C., Weaver, D., de la Fuente Perez, S., Bogorad, R., Koteliansky, V., Adijanto, J., Mootha, V. K., and Hajnóczky, G. (2013) MICU1 controls both the threshold and cooperative activation of the mitochondrial Ca(2)(+) uniporter. *Cell Metab.* **17,** 976–987
36. Baughman, J. M., Perocchi, F., Girgis, H. S., Plovanich, M., Belcher-Timme, C. A., Sancak, Y., Bao, X. R., Strittmatter, L., Goldberger, O., Bogorad, R. L., Koteliansky, V., and Mootha, V. K. (2011) Integrative genomics identifies MCU as an essential component of the mitochondrial calcium uniporter. *Nature* **476,** 341–345
37. Mallilankaraman, K., Cárdenas, C., Doonan, P. J., Chandramoorthy, H. C., Irrinki, K. M., Golenár, T., Csordás, G., Madireddi, P., Yang, J., Müller, M., Miller, R., Kolesar, J. E., Molgó, J., Kaufman, B., Hajnóczky, G., Foskett, J. K., and Madesh, M. (2012) MCUR1 is an essential component of mitochondrial Ca^{2+} uptake that regulates cellular metabolism. *Nat. Cell Biol.* **14,** 1336–1343
38. Sancak, Y., Markhard, A. L., Kitami, T., Kovács-Bogdan, E., Kamer, K. J., Udeshi, N. D., Carr, S. A., Chaudhuri, D., Clapham, D. E., Li, A. A., Calvo, S. E., Goldberger, O., and Mootha, V. K. (2013) EMRE is an essential component of the mitochondrial calcium uniporter complex. *Science* **342,** 1379–1382
39. Garlick, P. B., Soboll, S., and Bullock, G. R. (1992) Evidence that mitochondrial phosphate is visible in 31P NMR spectra of isolated, perfused rat hearts. *NMR Biomed.* **5,** 29–36
40. Garlick, P. B., Brown, T. R., Sullivan, R. H., and Ugurbil, K. (1983) Observation of a second phosphate pool in the perfused heart by 31P NMR; is this the mitochondrial phosphate? *J. Mol. Cell Cardiol.* **15,** 855–858
41. Paradies, G., and Ruggiero, F. M. (1991) Effect of aging on the activity of the phosphate carrier and on the lipid composition in rat liver mitochondria. *Arch. Biochem. Biophys.* **284,** 332–337
42. Harris, E. J., and Zaba, B. (1977) The phosphate requirement for Ca^{2+}-uptake by heart and liver mitochondria. *FEBS Lett.* **79,** 284–290
43. Leung, A. W., Varanyuwatana, P., and Halestrap, A. P. (2008) The mitochondrial phosphate carrier interacts with cyclophilin D and may play a key role in the permeability transition. *J. Biol. Chem.* **283,** 26312–26323
44. Litsky, M. L., and Pfeiffer, D. R. (1997) Regulation of the mitochondrial Ca^{2+} uniporter by external adenine nucleotides: the uniporter behaves like a gated channel which is regulated by nucleotides and divalent cations. *Biochemistry* **36,** 7071–7080